Directional Dark Matter Detection and Beyond: Diamond as a Platform for Mineral Detectors

Daniel Ang, Chinmay Bharathulwar, Priyanshu Bhattacharya, Mason Camp, Anson Cook, Gavishta Liyanage, Maximilian Shen, Jiashen Tang, Ronald Walsworth
Quantum Technology Center, University of Maryland

1 Introduction

Diamond is a monoatomic, wide-bandgap crystal that is both highly radiopure and hosts a versatile room-temperature quantum sensor in the nitrogen-vacancy (NV) center. These properties make it an attractive medium in which to detect and characterize nuclear-recoil damage tracks left by rare particle interactions. In particular, next-generation Weakly Interacting Massive Particle (WIMP) dark matter (DM) detectors will soon encounter the "neutrino fog," where solar-neutrino backgrounds obscure a DM signal [1]. Directional detection can overcome this limit by exploiting the differing angular distributions of neutrinos and WIMPs, rejecting backgrounds through imaging of nuclear-recoil damage tracks paired with conventional diamond-based real-time event detection [2–4]. Natural diamonds extend this reach into the past: with Gyr-scale exposure ages and intrinsic radiopurity, they are candidate paleodetectors in which optically stable color centers could record an integrated DM/neutrino dose over geological time [5]. More broadly, diamond is an ideal pathfinder mineral for the emerging program of mineral-based detection [6, 7]. Although less abundant than other mineral candidates such as quartz or olivine, it uniquely combines high-purity synthetic and well-characterized natural samples, a deep knowledge base of defects, color centers, and computational modeling, and the capability to host a highly versatile and developed NV quantum sensors that aid the study of track formation and morphology. Together, these features allow the readout and simulation techniques the field requires to be developed and experimentally validated in a single, well-understood material before being applied to other minerals.

Building on our contributions to previous MDνDMs [8, 9], we report recent progress at the ~~UMD QTC~~ on (i) multi-scale reconstruction of individual nuclear-recoil tracks, now reported in full in Ref. [10]; (ii) a maturing, mineral-agnostic simulation-and-inference toolchain; and (iii) a new natural-diamond paleodetection direction based on H3 centers.

2 Multi-scale reconstruction of single-ion tracks

We recently demonstrated multi-scale readout of individual sub-MeV nuclear-recoil tracks in nitrogen-rich diamond [10]. Single 800 keV carbon ions implanted at the Sandia National Laboratories microbeam facility produce spatially localized ensembles of NV centers after annealing, detected by confocal photoluminescence with a mean of 17.50 ± 0.38 NVs per ion across 222 sites. We then developed an experimentally calibrated forward model using SIIMPL [11] to model vacancy production during implantation followed by kinetic

Monte Carlo modelling of the annealing process which produces nitrogen-vacancy (NV) centers [12]. We found that applying a correction for second-nearest-neighbor defect reactions (discovered from first principles calculation) brings the predicted yield from ∼24 into agreement with the measured value (∼16.6). Crucially, head–tail directional information is partially retained through annealing and is recoverable by a simulation-based inference (SBI) [13] machine-learning (ML) classifier with ∼95% efficiency (correctly assigning head–tail direction for 95% of tracks) at a false-positive rate below 5%. The ML algorithm maintains similar directional reconstruction performance on simulated 100 keV tracks. Finally, spin-coherence measurements ($T_2 \approx 1.47\,\mu s$) indicate that nanoscale, magnetic-gradient NV imaging of the resulting tracks is feasible [4, 14]. Full details are given in Ref. [10].

Alongside this single-ion work, we are advancing several complementary efforts to develop novel methods for imaging damage tracks in diamond, including a light-sheet quantum diamond microscope (LS-QDM) [9] that adapts selective-plane fluorescence microscopy to NV-rich diamond for rapid, widefield three-dimensional imaging of the lattice strain imprinted by a recoil damage track [15]. With the first generation LS-QDM at the QTC, we have measured a light-sheet waist of ∼6.5 µm in diamond and demonstrated volumetric strain mapping in both isotopically purified and natural-abundance (^{13}C) synthetic diamond. Work is underway to refine the performance of the device and analyze the resulting 3D images of growth-induced strain structures.

3 Toward end-to-end event reconstruction in mineral detectors

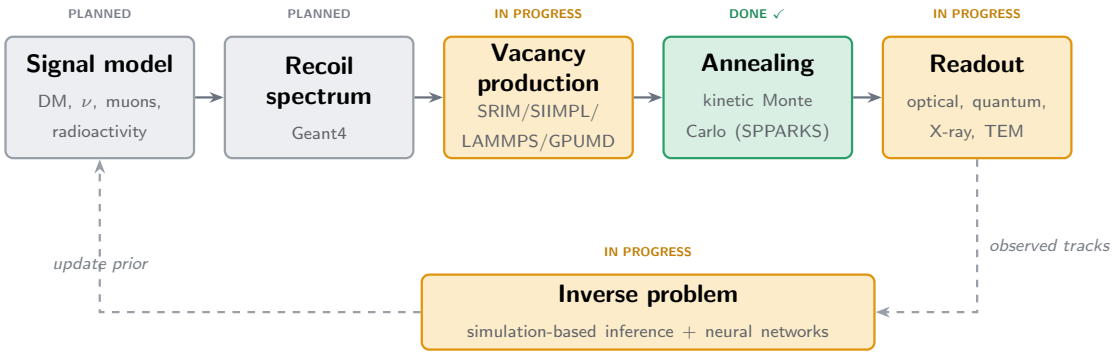


Figure 1: End-to-end simulation-and-inference pipeline for mineral track detection. A signal model and recoil spectrum (future work) feed vacancy production (binary-collision / molecular dynamics), defect annealing (kinetic Monte Carlo), and readout (optical, quantum, X-ray, TEM); the inverse problem is solved by simulation-based inference. Each stage can be applied to any candidate mineral.

A central goal is an end-to-end simulation pipeline that maps a signal model (dark matter, solar/atmospheric neutrinos, muons, and radiogenic backgrounds) to the damage tracks produced in mineral detectors and subsequently observed by diverse readout methods (Fig. 1). Such a forward simulation pipeline can then be utilized to address the inverse

problem, which provides the ability to analyze and interpret experimental data. At UMD, work has focused on developing forward simulations for vacancy production (using software packages such as SRIM, SIIMPL, and GPUMD), annealing (SPPARKS), and developing an SBI-based, ML-driven framework to solve the inverse problem. Other stages of the pipeline will be developed in tandem with other members of the MDDM collaboration, which UMD recently joined.

3.1 Forward modeling at scale with machine-learned molecular dynamics

Fully atomistic molecular dynamics simulation tools (MD) capture channeling, recombination, phonon transport, and other damage cascade phenemona that typical binary-collision codes such as Stopping and Range of Ions in Matter (SRIM) cannot. However, conventional MD methods are prohibitively slow for high-energy cascade work in diamond, requiring thousands of CPU hours per ∼10 keV track with typical codes such as LAMMPS [16]. We have transitioned to machine-learning-driven MD using the GPUMD package [17] with a neuroevolution potential (NEP) [18] trained on first-principles data [19] supplemented with close-range theory [20]. The potential reproduces DFT steady-state behaviors as benchmarked via elastic constants and energies (Table 1), and is supplemented with electronic stopping [21] and short-range nuclear stopping, enabling accurate modeling of cascade dynamics. Test runs show a ∼100× speedup that should enable recoil cascades up to ∼40 keV. Figure 2 shows some preliminary test cascades and the resulting vacancy statistics. This approach generalizes to any mineral, requiring only suitable DFT training data for less-studied materials.

Constant (GPa)	NEP (this work)	optB88-vdW DFT
C_{11}	1039	1061
C_{12}	127	126
C_{44}	557	559

Table 1: Elastic constants of diamond: NEP potential trained at UMD vs. DFT-based values (optB88-vdW).

3.2 Solving the inverse problem with simulation-based inference

To address the inverse problem, we use simulation-based inference (SBI) [13], training a neural posterior estimator on ∼200k SRIM-generated 3D tracks. Whereas Ref. [10] addressed only one-dimensional head–tail classification, here a geometric graph neural network (GVP-EGNN) [22] is capable of inferring both the energy and the recoil direction in full 3D. As shown in Fig. 3, this substantially outperforms conventional summary features (principal-component axis, longest string, centroid-to-centroid, vacancy count, track length), with the largest gains at low recoil energy where simple descriptors fail. Efforts are ongoing to refine the model to incorporate diamond crystal structure using SIIMPL [23] and the effects of finite track imaging resolution.

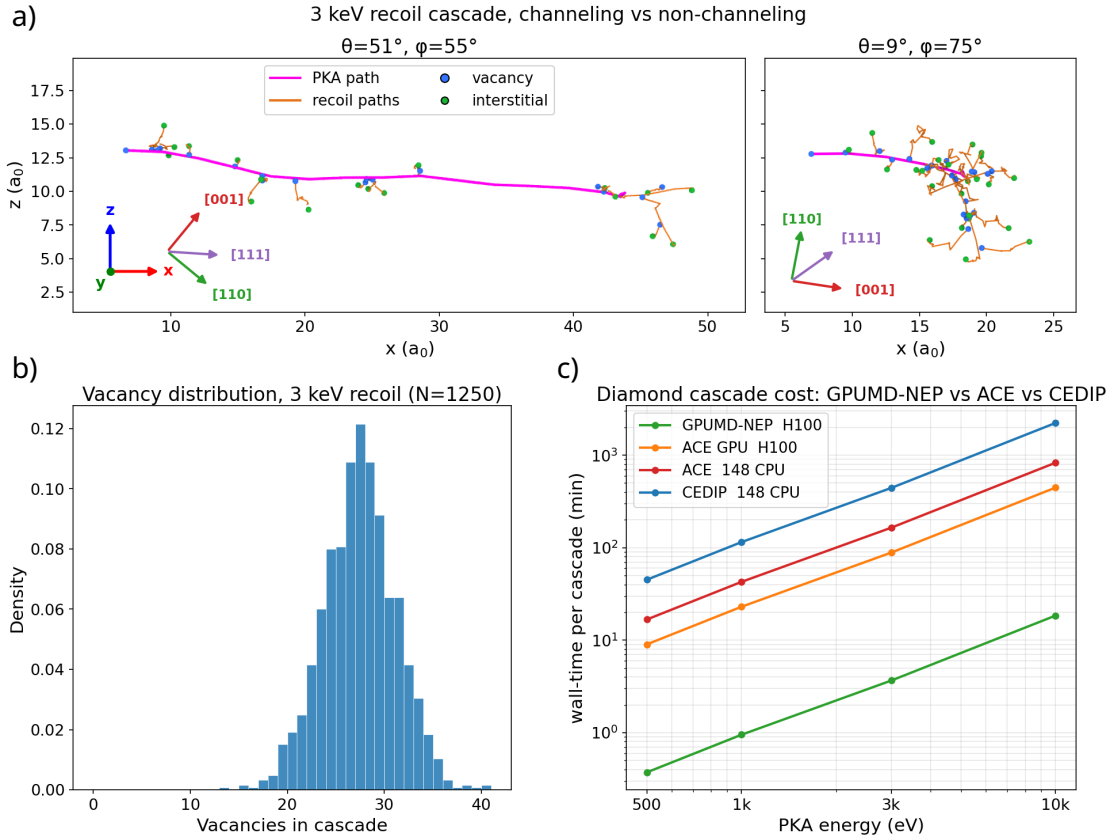


Figure 2: GPU-accelerated-MD (GPUMD) simulation of nuclear-recoil damage cascades in diamond. (a) representative vacancy distribution for a 3 keV recoil, with the crystal axes indicated; typical behaviors of both channeling and non-channeling cascades are shown. (b) distribution of the number of vacancies per cascade over N=1250 runs. (c) wall-time calculation cost for 0.5–10 keV cascades, showing how GPUMD enables simulating cascades beyond the reach of conventional MD.

4 Natural diamond as a paleodetector

While most mineral detection efforts at UMD have focused on synthetic diamond, natural diamond has recently emerged as an attractive paleodetection target. Diamonds typically reside in the mantle for ∼1–3 Gyr before kimberlite eruptions carry them to the surface, giving exposure times comparable to the oldest paleo-mineral candidates [24, 25]. The lattice is also intrinsically radiopure, with sub-ppb uranium abundances confined to inclusions rather than the lattice [5], while synthetic diamond is widely available for method development. The main challenges are the comparatively uranium-rich host kimberlite, which generates a radiogenic background [26], and deformation-induced defects which could mimic or obscure genuine recoil tracks.

The readout also differs from synthetic-diamond directional detection. NV readout requires isolated substitutional nitrogen (type Ib), which is rare in nature: over 95% of natural

diamonds are type Ia, with nitrogen aggregated into A-centers (2N) and B-centers (4N) [27]. We therefore propose the H3 (N–V–N) centre as the natural-diamond-compatible readout, formed when radiation-induced vacancies migrate during annealing and are trapped at A-centres [28]; mantle temperatures readily drive this migration, and the resulting centres are stable to temperatures exceeding 2000°C [29]. The calibrated track-formation framework of Sec. 3 and Ref. [10] can be extended to incorporate these constraints and predict H3 yields under geological thermal histories. At high ($\gtrsim 10^3$ ppm) nitrogen concentrations, however, H3 fluorescence is quenched by nearby aggregated nitrogen via a non-radiative energy-transfer process [28, 30], thus likely requiring filtering of candidate samples via FTIR screening. H3 centers are otherwise bright and photostable [31], rendering them promising for the light-sheet and super-resolution imaging being developed for color center readout; stimulated-emission-depletion imaging of single H3 centres has already been demonstrated [32, 33]. H3 centres thus merit experimental characterization in natural diamond to assess their suitability for paleodetection. As part of a preliminary study, we have obtained three natural diamond samples from De Beers containing H3 centres and plan to examine them with optical microscopy.

Acknowledgments

This work was supported by, or in part by, the Argonne National Laboratory under Award No. 2F60042; the DOE fusion program under Award No. DESC0021654; the U.S. Army Research Laboratory under Contract Nos. W911NF1920181 and W911NF2420143; the LPS/QTC Jumping Electron Fellowship through award H9823022C0029; and the University of Maryland Quantum Technology Center.

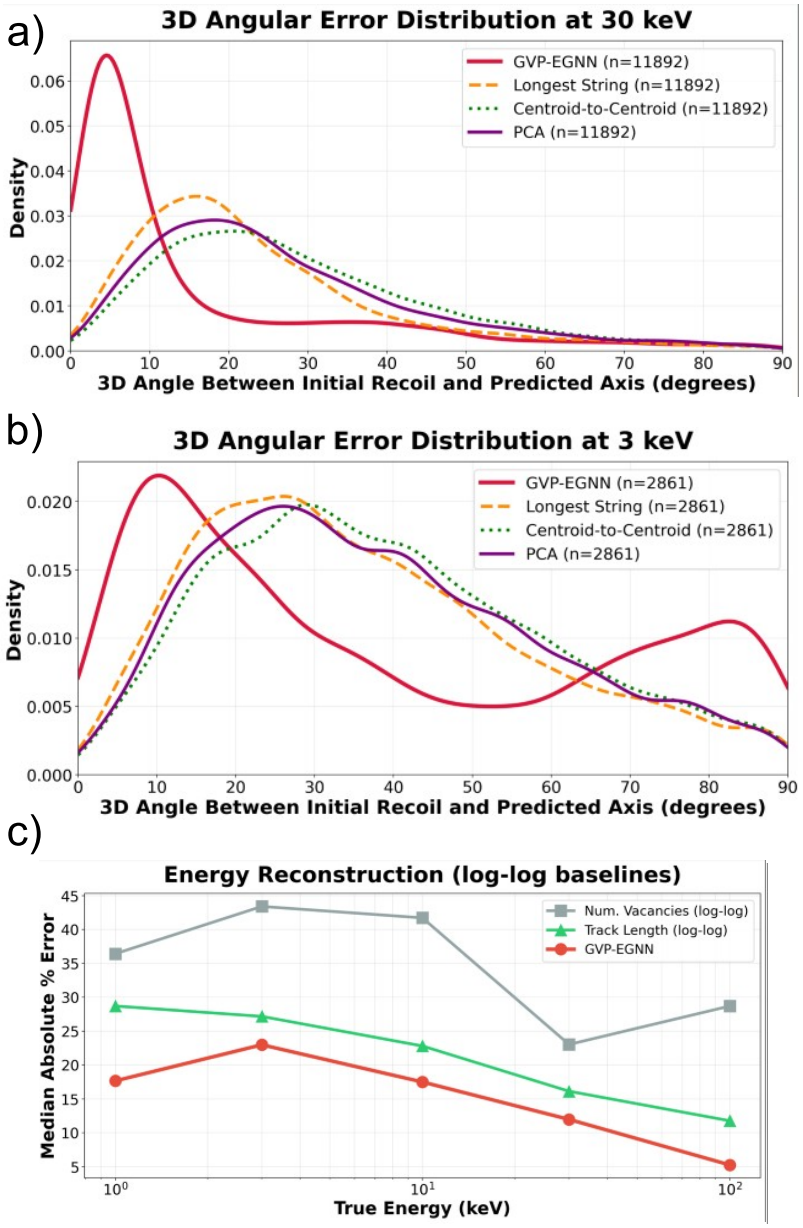


Figure 3: Simulation-based-inference reconstruction of recoil direction and energy from 3D vacancy distributions, using SRIM-generated tracks. (a, b) Distribution of the 3D angle between the true recoil axis and the predicted axis, for the GVP-EGNN model compared to three classical summary-feature baselines (longest string, centroid-to-centroid, principal component analysis), at (a) 30 keV and (b) 3 keV recoil energy. GVP-EGNN is sharply peaked at small angles in both cases, though at 3 keV it exhibits a secondary peak near 80° that is still under investigation. (c) Median absolute percent error in energy reconstruction as a function of true recoil energy, comparing GVP-EGNN to two classical baselines (number of vacancies, track length). GVP-EGNN outperforms both across the full energy range, with the largest relative gains at low energy.

References

[1] C. A. J. O'Hare, *New Definition of the Neutrino Floor for Direct Dark Matter Searches*, *Physical Review Letters* **127** (Dec., 2021) 251802.

[2] S. Rajendran, N. Zobrist, A. O. Sushkov, R. Walsworth and M. Lukin, *A method for directional detection of dark matter using spectroscopy of crystal defects*, *Physical Review D* **96** (Aug., 2017) 035009.

[3] M. C. Marshall, M. J. Turner, M. J. H. Ku, D. F. Phillips and R. L. Walsworth, *Directional detection of dark matter with diamond*, *Quantum Science and Technology* **6** (Mar., 2021) 024011.

[4] R. Ebadi, M. C. Marshall, D. F. Phillips, J. Cremer, T. Zhou, M. Titze et al., *Directional detection of dark matter using solid-state quantum sensing*, *AVS Quantum Science* **4** (Nov., 2022) 044701.

[5] J. D. Kramers, *Lead, uranium, strontium, potassium and rubidium in inclusion-bearing diamonds and mantle-derived xenoliths from Southern Africa*, *Earth and Planetary Science Letters* **42** (Jan., 1979) 58–70.

[6] S. Baum, P. Stengel, N. Abe, J. F. Acevedo, G. R. Araujo, Y. Asahara et al., *Mineral detection of neutrinos and dark matter. A whitepaper*, *Physics of the Dark Universe* **41** (Aug., 2023) 101245.

[7] A. K. Drukier, S. Baum, K. Freese, M. Górski and P. Stengel, *Paleo-detectors: Searching for dark matter with ancient minerals*, *Physical Review D* **99** (Feb, 2019) 043014.

[8] D. G. Ang, X. Liu, J. Tang, M. Shen, R. Ebadi and R. Walsworth, *Progress toward a solid-state directional dark matter detector*, in *MDvDM 2024 Proceedings*, pp. 18–21, 2024, DOI.

[9] D. G. Ang, J. Tang, M. Shen, M. Camp, A. Gilpin, G. Liyanage et al., *Progress toward a solid-state directional dark matter detector*, in *MDvDM 2025 Proceedings*, pp. 18–21, 2025, DOI.

[10] D. G. Ang, J. Tang, M. Shen, M. Titze, G. Liyanage, J. Chapman et al., *Multi-scale reconstruction of single-ion damage tracks in diamond via nitrogen-vacancy centers*, June, 2026. 10.48550/arXiv.2606.23621.

[11] M. S. Janson, *Hydrogen diffusion and ion implantation in silicon carbide*, Ph.D. thesis, KTH-Royal Institute of Technology, 2003.

[12] J. A. Mitchell, F. Abdeljawad, C. Battaile, C. Garcia-Cardona, E. A. Holm, E. R. Homer et al., *Parallel simulation via SPPARKS of on-lattice kinetic and Metropolis Monte Carlo models for materials processing*, *Modelling and Simulation in Materials Science and Engineering* **31** (2023) 055001.

[13] A. Tejero-Cantero, J. Boelts, M. Deistler, J.-M. Lueckmann, C. Durkan, P. J. Gonçalves et al., *SBI – A toolkit for simulation-based inference*, July, 2020. 10.48550/arXiv.2007.09114.

[14] H. Zhang, K. Arai, C. Belthangady, J.-C. Jaskula and R. L. Walsworth, *Selective addressing of solid-state spins at the nanoscale via magnetic resonance frequency encoding*, *npj Quantum Information* **3** (Aug., 2017) 1–8.

[15] M. C. Marshall, R. Ebadi, C. Hart, M. J. Turner, M. J. Ku, D. F. Phillips et al.,

High-Precision Mapping of Diamond Crystal Strain Using Quantum Interferometry, *Physical Review Applied* **17** (2022) 024041.

[16] A. P. Thompson, H. M. Aktulga, R. Berger, D. S. Bolintineanu, W. M. Brown, P. S. Crozier et al., *LAMMPS - a flexible simulation tool for particle-based materials modeling at the atomic, meso, and continuum scales*, *Computational Physics Communications* **271** (2022) 108171.

[17] Z. Fan, Y. Wang, P. Ying, K. Song, J. Wang, Y. Wang et al., *GPUMD: A package for constructing accurate machine-learned potentials and performing highly efficient atomistic simulations*, *The Journal of Chemical Physics* **157** (09, 2022) 114801.

[18] Z. Fan, Z. Zeng, C. Zhang, Y. Wang, K. Song, H. Dong et al., *Neuroevolution machine learning potentials: Combining high accuracy and low cost in atomistic simulations and application to heat transport*, *Phys. Rev. B* **104** (Sep, 2021) 104309.

[19] P. Rowe, V. L. Deringer, P. Gasparotto, G. Csányi and A. Michaelides, *An accurate and transferable machine learning potential for carbon*, *The Journal of Chemical Physics* **153** (2020) 034702.

[20] K. Nordlund, S. Lehtola and G. Hobler, *Repulsive interatomic potentials calculated at three levels of theory*, *Physical Review A* **111** (2025) 032818.

[21] F. Bivort Haiek, A. M. P. Mendez, C. C. Montanari and D. M. Mitnik, *ESPNN: A novel electronic stopping power neural-network code built on the IAEA stopping power database. i. atomic targets*, *Journal of Applied Physics* **132** (12, 2022) 245103.

[22] B. Jing, S. Eismann, P. A. Suriana, R. J. L. Townshend and R. O. Dror, *Learning from protein structure with geometric vector perceptrons*, in *International Conference on Learning Representations (ICLR)*, 2021.

[23] M. S. Janson, "SIIMPL: Simulation of Ion IMPLantation." `https://github.com/msjanson01/siimpl`, 2022.

[24] J. J. Gurney, H. H. Helmstaedt, S. H. Richardson and S. B. Shirey, *Diamonds through time*, *Economic Geology* **105** (2010) 689–712.

[25] K. V. Smit and S. B. Shirey, *How old are diamonds? are they forever?*, *Gems & Gemology* **55** (2019) 102–109.

[26] P. Kresten, *Uranium in kimberlites and associated rocks, with special reference to Lesotho occurrences*, *Lithos* **7** (1974) 171–180.

[27] C. M. Breeding and J. E. Shigley, *The "type" classification system of diamonds and its importance in gemology*, *Gems & Gemology* **45** (2009) 96–111.

[28] M. D. Crossfield, G. Davies, A. T. Collins and E. C. Lightowlers, *The role of defect interactions in reducing the decay time of H3 luminescence in diamond*, *Journal of Physics C: Solid State Physics* **7** (May, 1974) 1909.

[29] C. M. Breeding, S. Eaton-Magaña and J. E. Shigley, *Natural-color green diamonds: A beautiful conundrum*, *Gems & Gemology* **54** (2018) 2–27.

[30] A. T. Collins, *The colour of diamond and how it may be changed*, *Journal of Gemmology* **27** (2001) 341–359.

[31] A. Pant, C. Gupta, K. Senkalla, G. Felsted, X. Xia, T. Spohn et al., *Reduced photothermal*

heating in diamonds enriched with H3 point defects, *Journal of Applied Physics* **131** (2022) 234401.

[32] R. Kolesov, S. Lasse, C. Rothfuchs, A. D. Wieck, K. Xia, T. Kornher et al., *Superresolution microscopy of single rare-earth emitters in YAG and H3 centers in diamond*, *Physical Review Letters* **120** (2018) 033903.

[33] G. Laporte and D. Psaltis, *STED imaging of green fluorescent nanodiamonds containing nitrogen-vacancy-nitrogen centers*, *Biomedical Optics Express* **7** (2016) 34–44.